LEGENDS FOR SUPPLEMENTARY FIGURES

Figure 1. (A) Multiple sequence alignment of the N-terminal (residues 1-383) of MVP proteins. *Mus musculus* (Mm, accession number NP542369), *Homo sapiens* (Hs, accession number NP059447) Xenopus laevis (Xs, accession number NP001079939) *Danio rerio* (Dr, accession number NP958482) *Strongylocentrotus purpuratus* (Sp, accession number NP001116989). The strictly conserved residues are shown as red blocks and white characters and similar residues are shown in blue boxes and red characters. Secondary structure definitions, as determined in the crystal structure of R1-R7 are drawn above the sequence alignment. The predicted calcium binding regions of repeats R3 and R4 are marked by green bars below the sequence. (B) View of the α-carbon trace in the R1-R7 structure with every tenth residues numbered. (C) Molecular surface of R1-R7 represented with the electrostatic potential, in blue and red for the positive and negative charges, respectively. The electrostatic potential was calculated and rendered with PyMOL (DeLano, 2002), with colouring levels ranging from –56.8 to 56.8. Two consecutive molecules in the P1 crystal packing are shown. A close-up of the electronegative surface of repeats R3 and R4 is depicted at the right side, with the acidic residues explicitly labeled. This surface would form the predicted binding site of Ca^{2+} ions and PTEN.

Figure 2 Crystal packing of the vault particles in the C2 unit cell. (A) Packing is represented in the ac (left) and ab (right) planes. (B) Details of the intermolecular contacts, considering rings of different numbers of copies of the R1R7 fragment. No direct interactions are found when 38 copies are considered (left) and models with rotational symmetries of 40 or higher result in steric clashes (right). A rotational symmetry of 39 allows optimal interactions between neighbor vault particles.

Figure 3 Thirty nine fold averaged density of the vault particle at 8 Å resolution. Side (a) and top (b) views of the electron density. Close-up pictures of the electron density around the R1-R7 (c) and the α-helical domain regions (d), with the Cα models placed inside.

Figure 4 Secondary structural elements of MVP identified in the 8 Å averaged density of the vault particle. These secondary structure features were identified and modeled

using the AIRS programs (Baker et al., 2007), which provides a graphic interface to the SSEHunter and SSEbuilder programs in the Chimera visualization software package (Pettersen et al., 2004) The vault particle is represented by cylinders (α-helices, yellow) and planks (β-sheets, blue). Top (left) and side (right) views are shown.

Figure 5 Density correlation plots corresponding to the R1R7 region (residues 1-380) in the structures of: (A) crystal form P1 of the R1R7 fragment, (B) the 3.5 Å of the entire vault particle (Tanaka et al., 2009).

Figure 6 Stereoview of a simulated annealing Fo-Fc omit map (contoured at 3.0 σ) around the β2- β3 loops of R1 and R2 domains of the R1-R7 structure (P1 crystal form)., The model is placed inside in ball and stick representation colored in atom type code. Names for the N- and C-terminal residues of each loop are labeled.

Figure 7 View of the R1-R7 packing interactions, conserved in all three crystals forms. Asp39 of R1 appears protonated, interacting with the peptide oxygen of Gly354 of the neighbouring R7. In addition, residues Ile7 and Ile36 are involved in hydrophobic contacts with Leu358.

Figure 8 Plot of the reciprocal space layer h=0, showing the severe anisotropy in the data. Intensity is represented by the size of the reflections. The figure was prepared with the program XPREP (BRUKER AXS).

Figure 9. Self-rotation function (180º section), calculated from the 8 Å diffraction data of the of the $P2_1$ vault crystals. The function was calculated with program MOLREP (CCP4, 1994).

REFERENCES

Baker, M.L., Ju, T. and Chiu, W. (2007) Identification of secondary structure elements in intermediate-resolution density maps. *Structure*, 15, 7-19.

CCP4 (1994) The CCP4 suite: programs for protein crystallography. *Acta Crystallogr D Biol Crystallogr*, 50, 760-763.

DeLano, W.L. The PyMOL Molecualr Graphics System (DeLano Scientific, San Carlos, California, USA, 2002).

Pettersen, E.F., Goddard, T.D., Huang, C.C., Couch, G.S., Greenblatt, D.M., Meng, E.C. and Ferrin, T.E. (2004) UCSF Chimera--a visualization system for exploratory research and analysis. *J Comput Chem*, 25, 1605-1612.

Tanaka, H., Kato, K., Yamashita, E., Sumizawa, T., Zhou, Y., Yao, M., Iwasaki, K., Yoshimura, M. and Tsukihara, T. (2009) The structure of rat liver vault at 3.5 angstrom resolution. *Science*, 323, 384-388

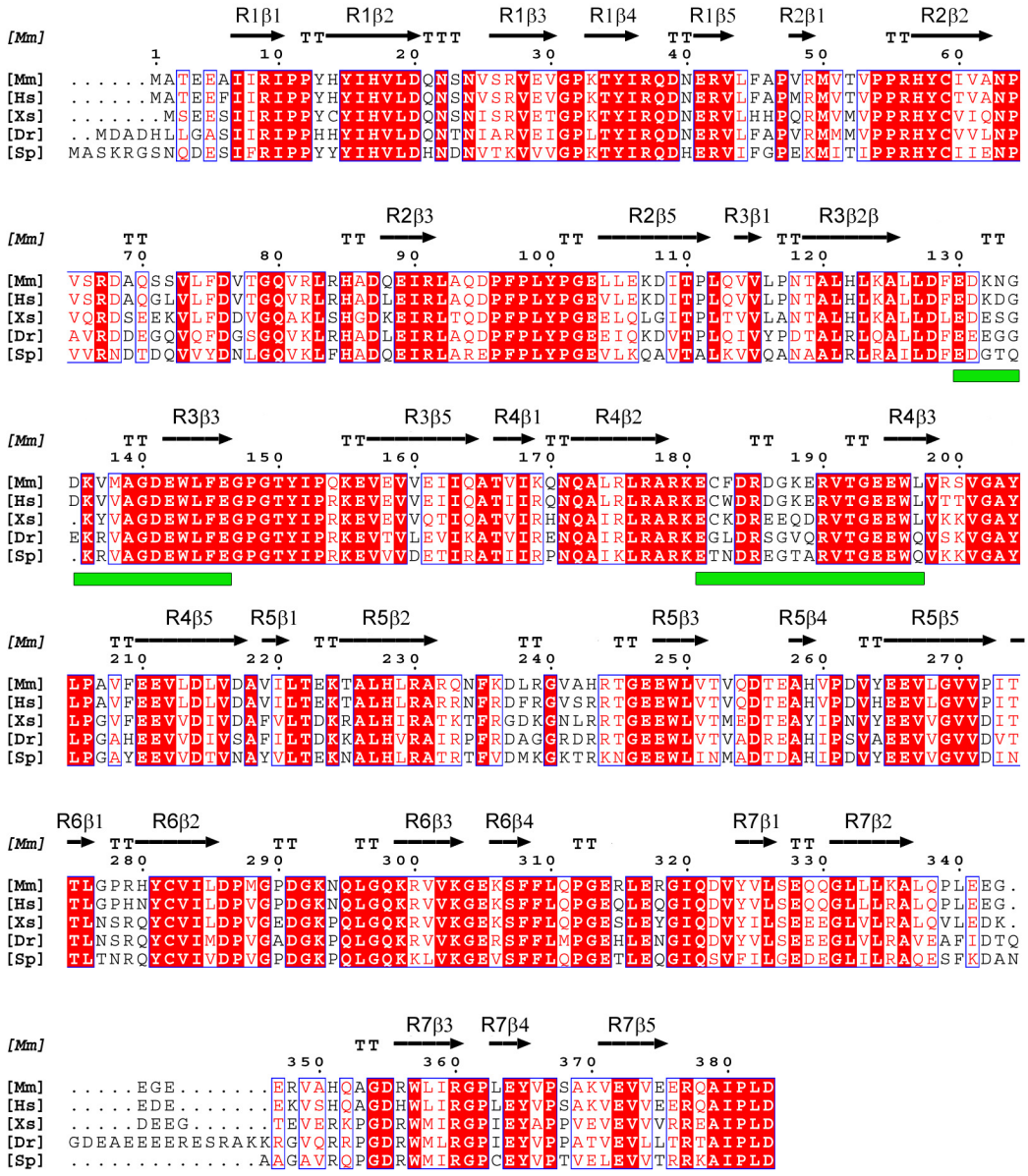
R1β1 R1β2 R1β3 R1β4 R1β5 R2β1 R2β2
R2β3 R2β5 R3β1 R3β2β
R3β3 R3β5 R4β1 R4β2 R4β3
R4β5 R5β1 R5β2 R5β3 R5β4 R5β5
R6β1 R6β2 R6β3 R6β4 R7β1 R7β2
R7β3 R7β4 R7β5
[Mm]
[Hs]
[Xs]
[Dr]
[Sp]

SI: Figure1A

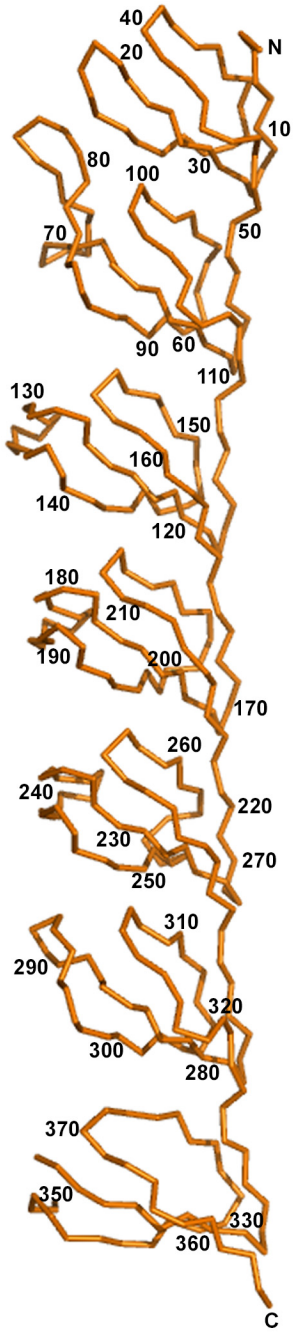
40
20
N
10
80
100
30
70
50
90
60
110
130
150
160
140
120
180
210
190
200
170
260
240
220
230
270
250
310
290
320
300
280
370
350
330
360
C

SI: Figure1B

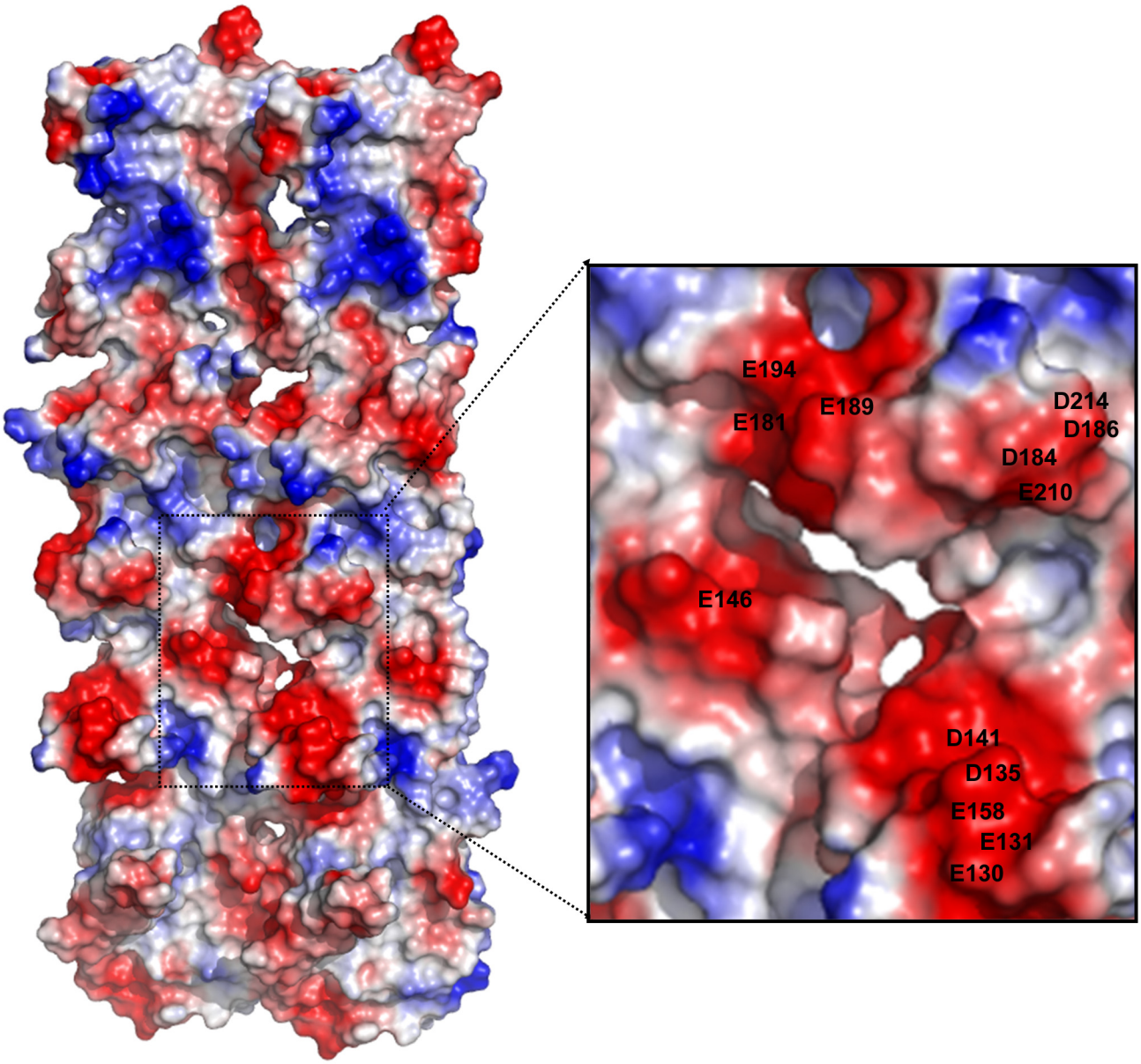
E194
E189
E181
D214
D186
D184
E210
E146
D141
D135
E158
E131
E130

SI: Figure1C

A

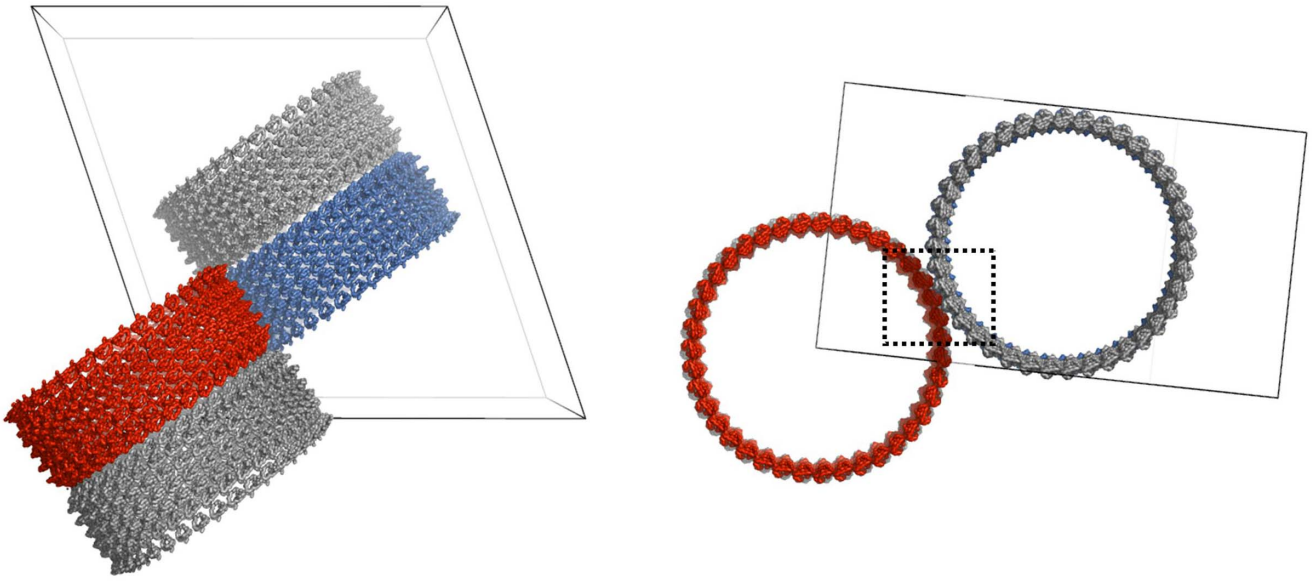

B

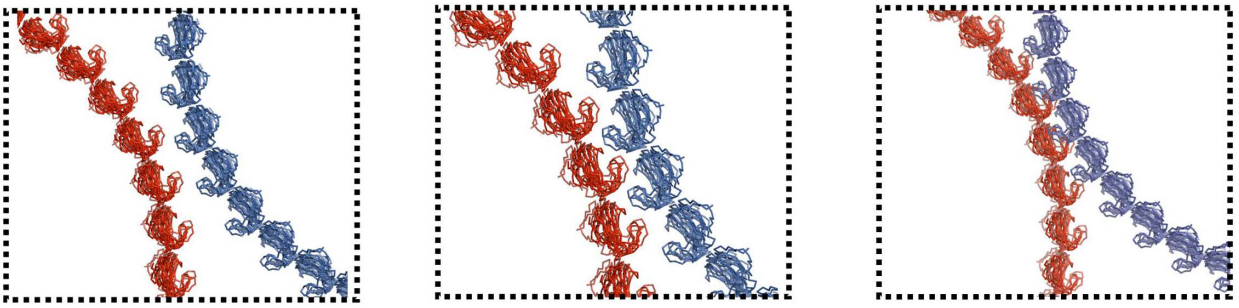

D38 D39 D40

SI: Figure 2

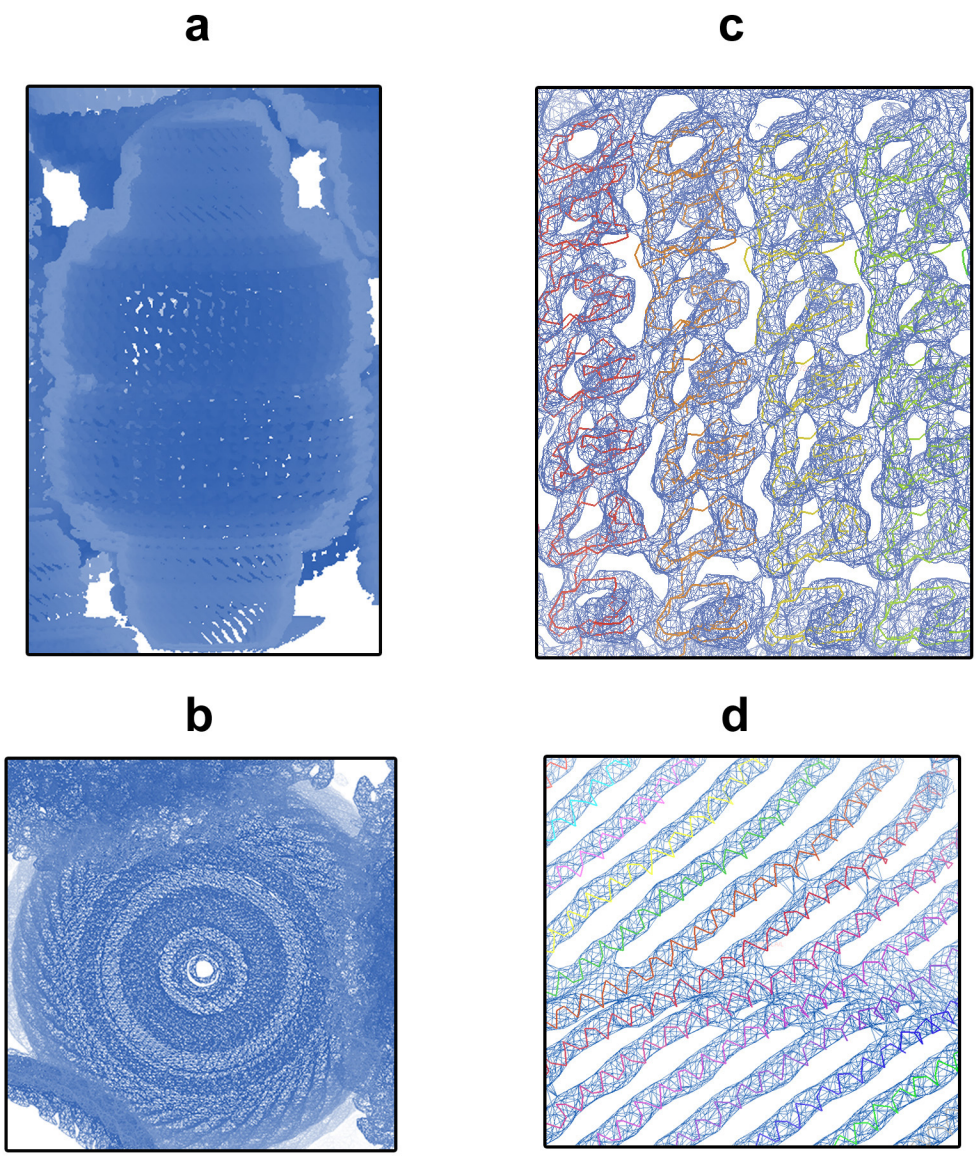

SI: Figure 3

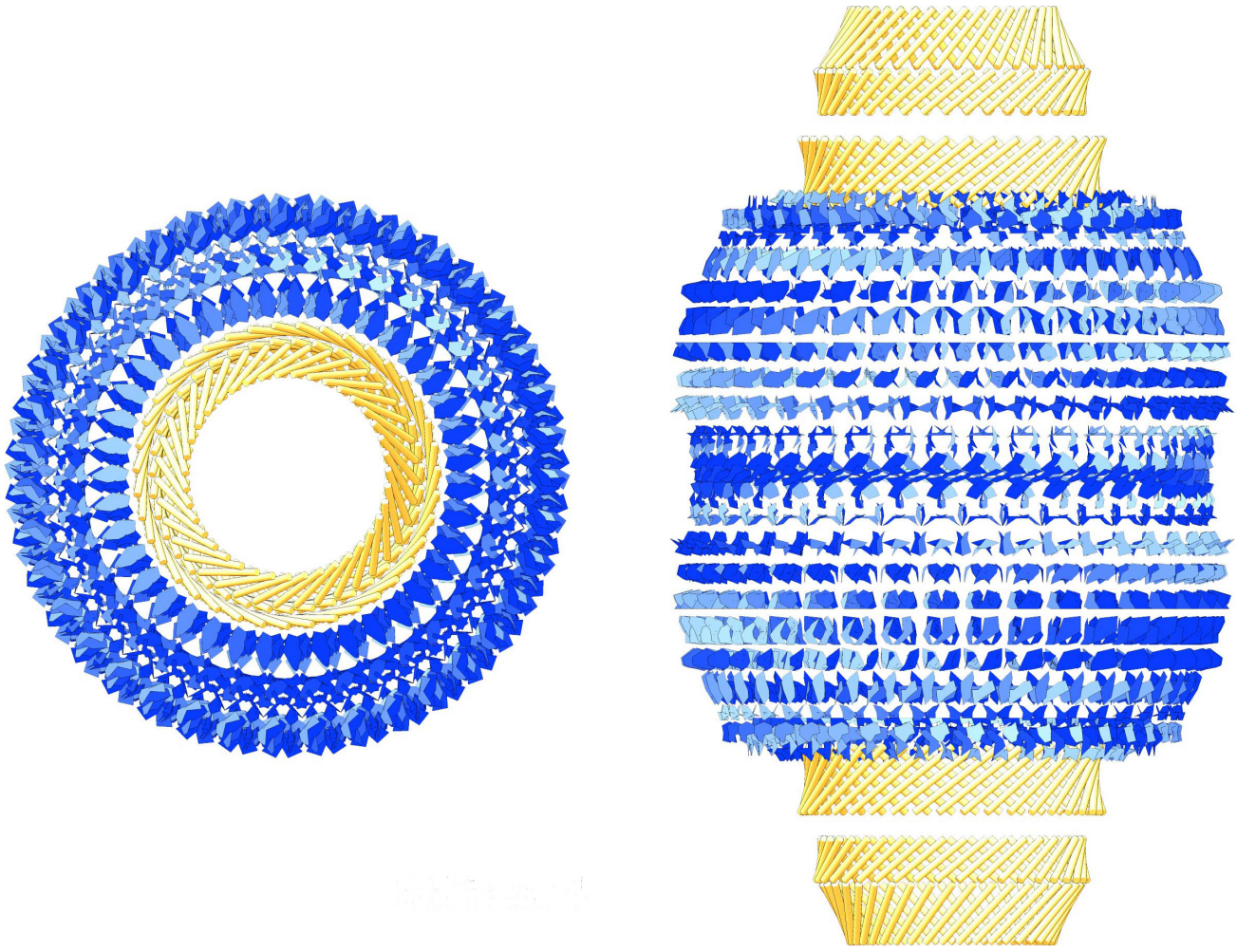

SI: Figure 4

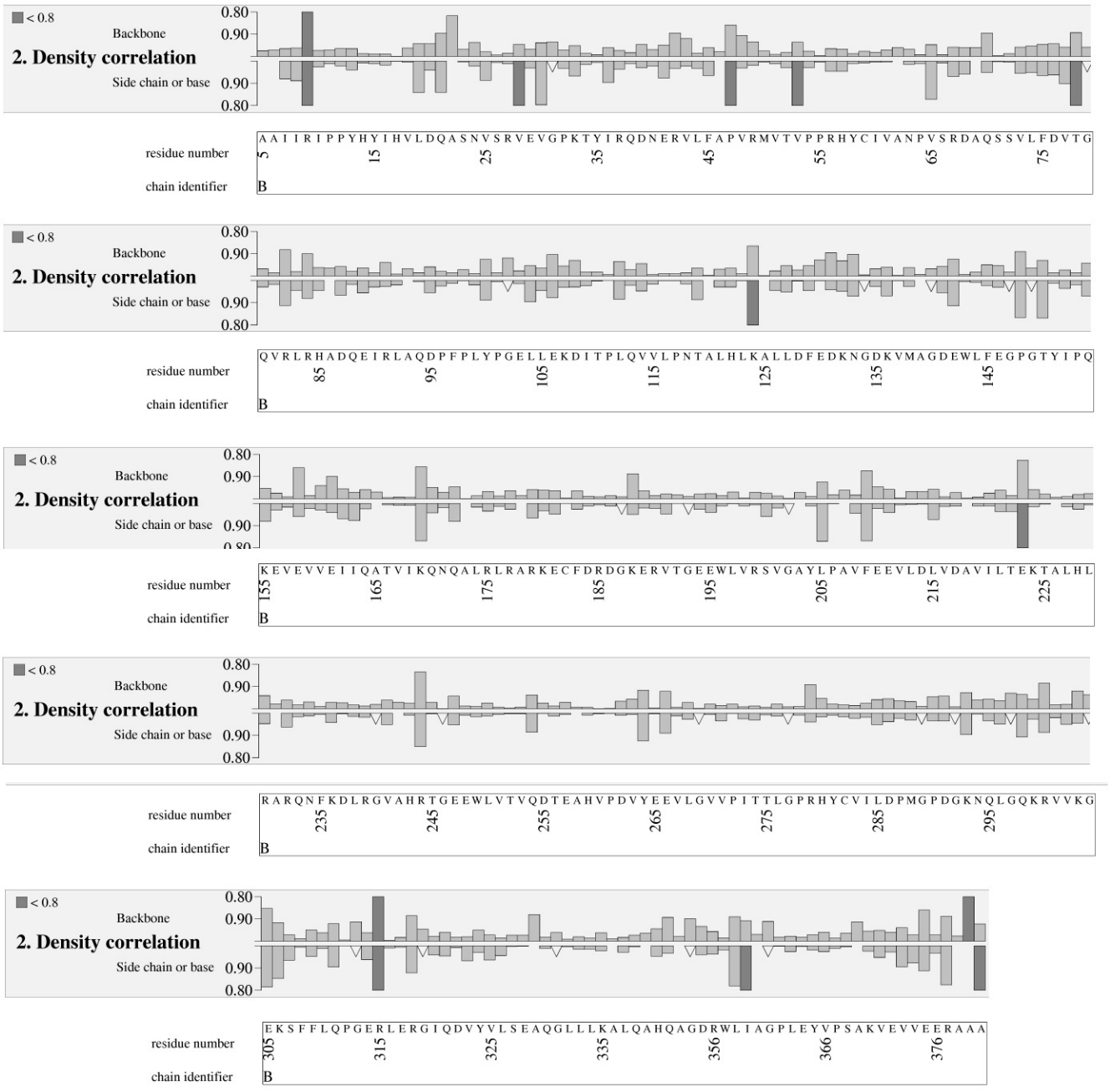
< 0.8
Backbone
2. Density correlation
Side chain or base
0.80
0.90
0.90
0.80
residue number
chain identifier
B

SI:Figure 5A

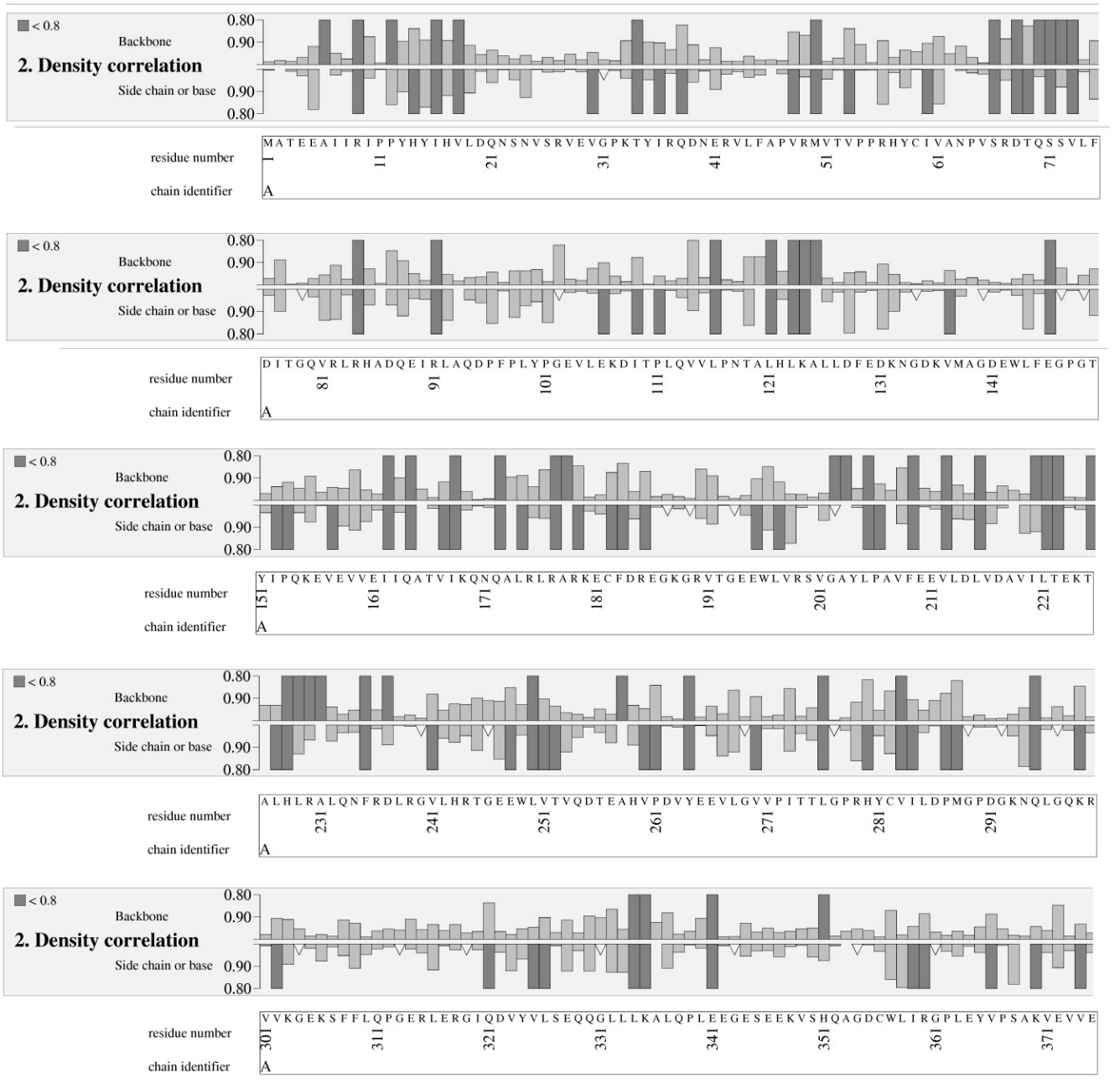
< 0.8
Backbone
2. Density correlation
Side chain or base
0.80
0.90
0.90
0.80
residue number
chain identifier
A
M A T E E A I I R I P P Y H Y I H V L D Q N S N V S R V E V G P K T Y I R Q D N E R V L F A P V R M V T V P P R H Y C I V A N P V S R D T Q S S V L F
D I T G Q V R L R H A D Q E I R L A Q D P F P L Y P G E V L E K D I T P L Q V V L P N T A L H L K A L L D F E D K N G D K V M A G D E W L F E G P G T
Y I P Q K E V E V V E I I Q A T V I K Q N Q A L R L R A R K E C F D R E G K G R V T G E E W L V R S V G A Y L P A V F E E V L D L V D A V I L T E K T
A L H L R A L Q N F R D L R G V L H R T G E E W L V T V Q D T E A H V P D V Y E E V L G V V P I T T L G P R H Y C V I L D P M G P D G K N Q L G Q K R
V V K G E K S F F L Q P G E R L E R G I Q D V Y V L S E Q Q G L L L K A L Q P L E E G E S E E K V S H Q A G D C W L I R G P L E Y V P S A K V E V V E

SI:Figure 5B

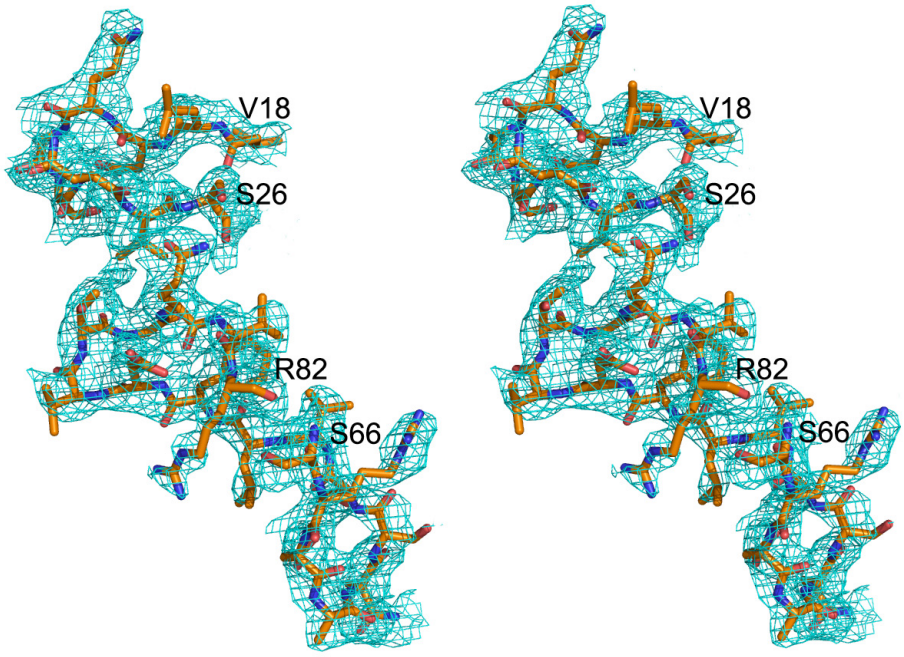

SI:Figure 6

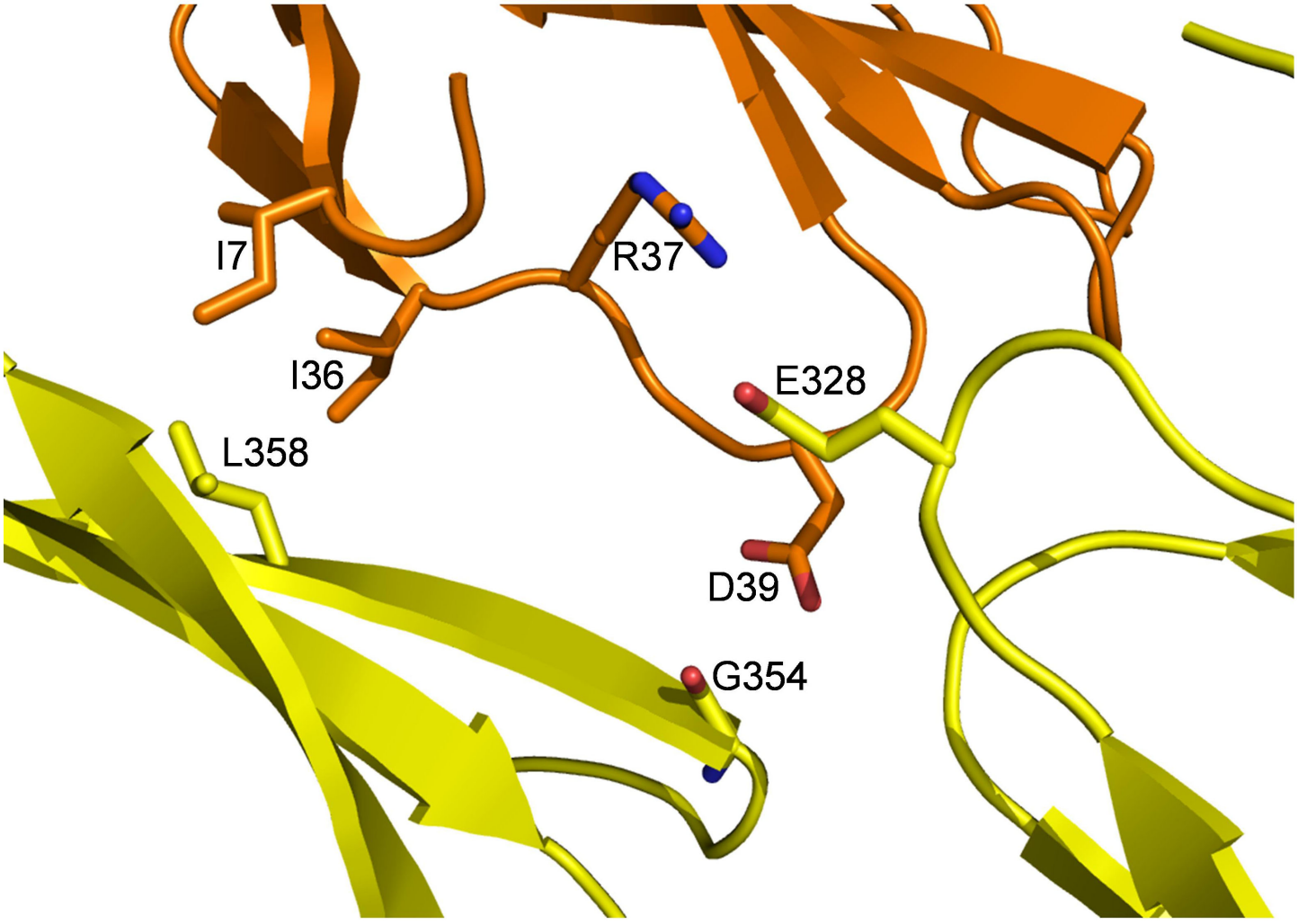

SI:Figure 7

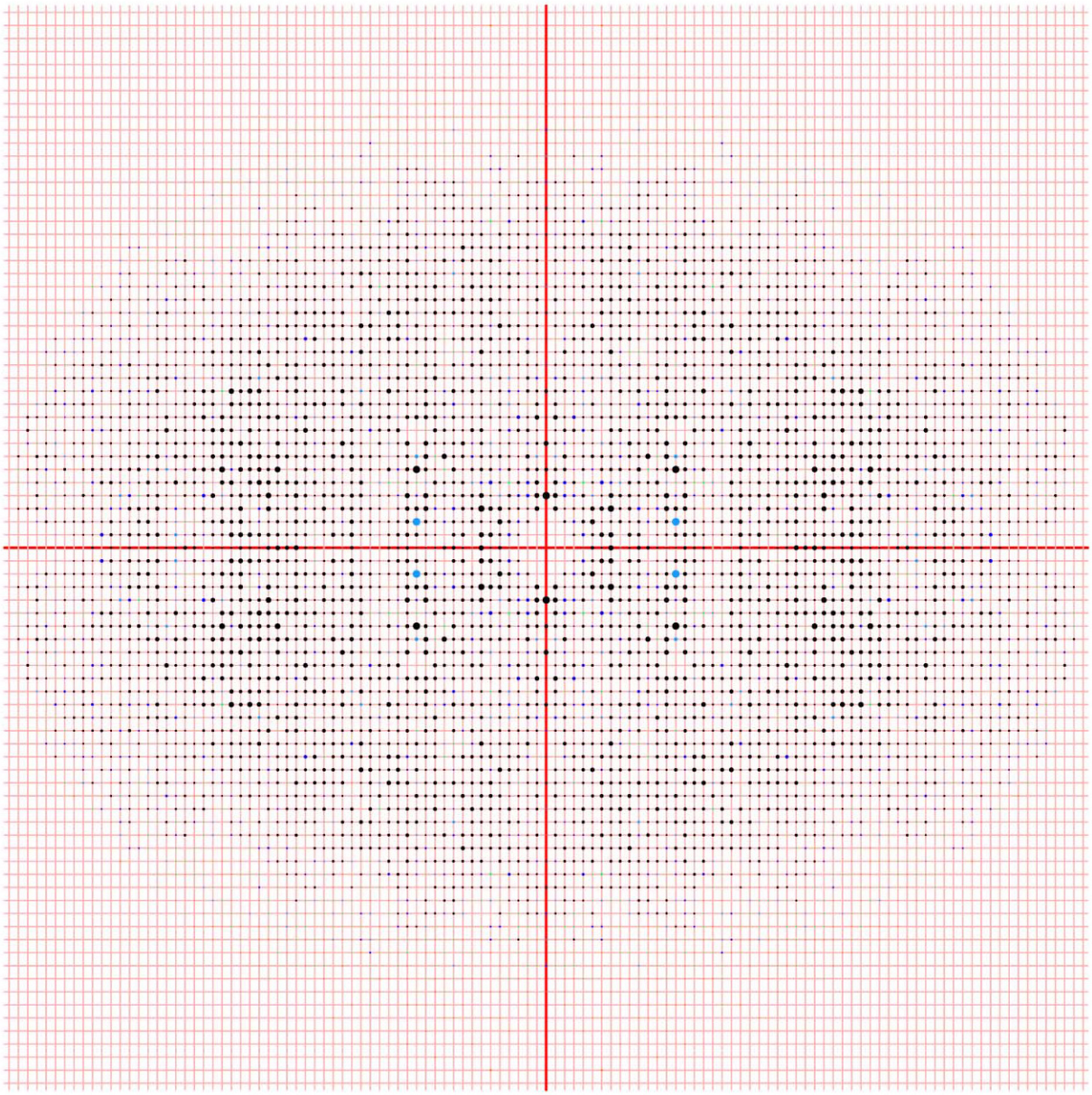

SI:Figure 8

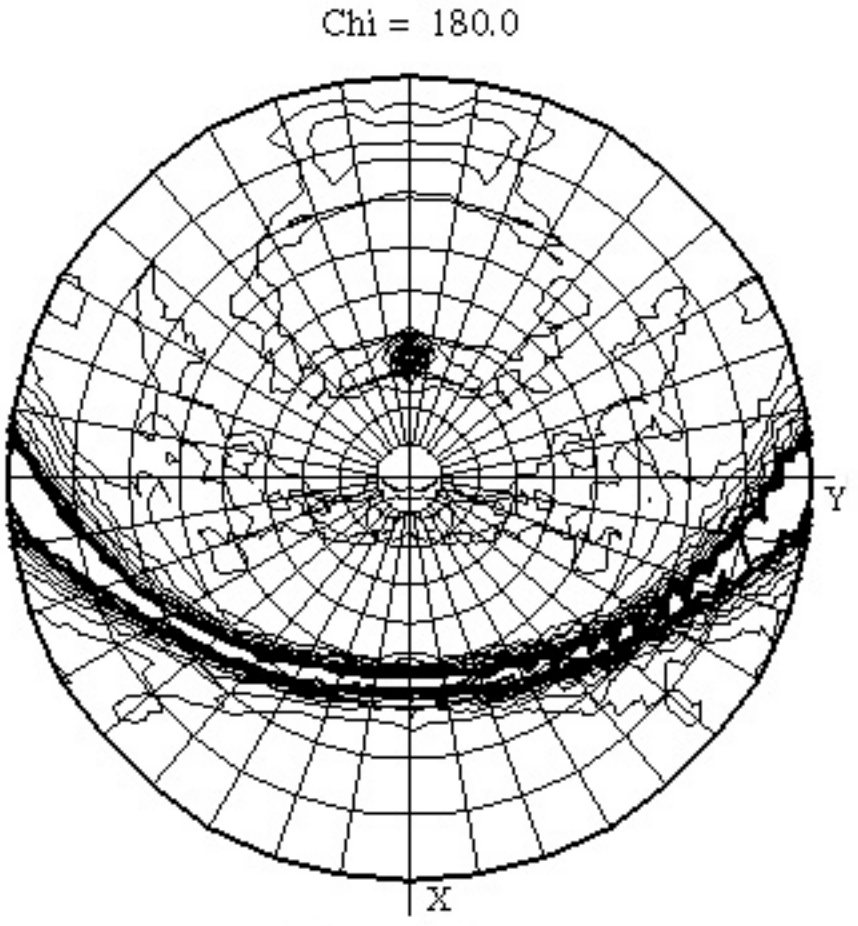

SI: Figure 9

Supplementary Methods

X-ray analysis of the vault particle

Two different crystal forms were analysed: first crystals were monoclinic, space group C2, with unit cell parameters a_C=726.2Å, b_C=391.4Å, c_C=607.6Å and β_C=124.1° . The second type of crystals were also monoclinic, space group $P2_1$, with unit cell parameters a_P=601.1Å, b_P=386.6Å, c_P=627.1Å and β_P=108.6°

Both, $P2_1$ and C2, unit cells have similar volumes and their cell axis can be related as: $\vec{\mathbf{a}}_C \approx \vec{\mathbf{a}}_P + \vec{\mathbf{c}}_P$; $\vec{\mathbf{b}}_C \approx \vec{\mathbf{b}}_P$ and $\vec{\mathbf{c}}_C \approx -\vec{\mathbf{a}}_P$.

The self-rotation functions, calculated at 10 Å resolution with the program MOLREP, showed for both crystal forms the same, very unique, features (Supplementary Figure 9): i) A sharp and strong peak in the a c plane, which remains dominant for essentially all κ values (named henceforth the vaults rotational symmetry peak along the longest vault axis) and ii) A prominent continuous streak, in the κ=180° section, that is located in the plane perpendicular to the strong peak and, consequently, also to the a c plane. The similarities of these characteristic features indicate closely related packing of the vault particles in both crystal forms, even despite the different crystallographic parameters. For the C2 crystals, a half vault particle can be placed in the asymmetric unit with the two halves of a vault related by a crystallographic two fold, as showed in the recently reported structure (Tanaka et al., 2009). For the $P2_1$ crystals, with a strong peak in the native Patterson function at (0.5, 0.5, 0.5), the asymmetric unit can contain a whole vault particle, with its centre in (0.25, Y, 0.25), that would be related to a second vault particle in the unit cell by the crystal 2_1 symmetry. The translation between the centres of both particles corresponds to the Patterson peak. Therefore, the compact packing of vault particles is almost identical in both crystal forms In fact, in the $P2_1$ cell only small deviation from the C2 packing should be expected because reflexions with h+k+l odd are absent or very weak (pseudo-body centred) till about 15 Å resolution. These observations could explain, at least in part, the easiness of the interconvertibility observed among different crystals forms.

SI. Table I
R1-R7 Interdomain contacts

R1-R2	R2-R3	R3-R4	R4-R5	R5-R6	R6-R7
Y13-M50	L112-Q113	N118-A203	A173-V260	I273-T274	V323-Y324
H14-M50	-V114	-L205	R175-V263	-S307	-E364
Y15-P98	L92-I152	T119-L205	R190-Y264	-F308	-Y365
H17-P101	I90-P153	A120-L205	E195-V263	T225-F309	D322-Y324
-Y100	Y58-P153	H122-V208	W196-V263	K224-F309	R279-E364
-L99	L112-P153	E142-V208	L197-D262	A226-F309	Y281-P367
N24-Q80	I90-P153	I163-L205	L197-V263	P272-F309	V301-P367
V25-G79	-P154	N164-L205	-P261	T222-F309	
-Q80	Q88-K155	A165-L205	R199-D262	V271-L310	
S26-Q80	I90-K155	-A203	-V260	L250-L310	
-P101	E89-K155	-Y204	V216-V260	-L311	
R27-P101	I90-K155	-V167	-P261	-P312	
V28-Y100	Q88-K155	-T166	D217-V219	H228-P312	
-P98	R84-K155		A218-V219	W249-P312	
V48-Met50			-V260		
R49-Met50			-H259		
-V51			-A258		
			-I220		

SI. Table II. Data collection statistics of vault crystals

Data collection	**$P2_1$**	**C2**
Wavelength(Å)	0.979	0.979
Resolution(Å)	80-8 (8.5-8.0)	60-10 (10.5-10)
Space group	**P_{21}**	C2
Unit cell(Å)	a=601.1 b=386.6 c=627.1 β=108.6	a=726.2 b=391.4 c=607.6 β=124.1
Total data	925949	158973
Unique data	158528	38094
Mean (<I/σ>)	5.6 (1.5)	3.1 (0.8)
$R_{merge\ \%}$	18.2 (38.3)	17.9 (60.3)
Completeness (%)	50.1 (27.7)	48.0 (40.1)

Values in parenthesis are for the highest resolution shell